

# The magneto-optical effect of cold atoms in an integrating sphere for atomic clock and optical magnetometer

Jinyin Wan,<sup>1</sup> Huadong Cheng,<sup>1,\*</sup> Yanling Meng,<sup>1</sup> Ling Xiao,<sup>1</sup>  
Peng Liu,<sup>1</sup> Xiumei Wang,<sup>1</sup> Yanning Wang,<sup>1</sup> and Liang Liu<sup>1,†</sup>

<sup>1</sup>Key Laboratory of Quantum Optics, Shanghai Institute of Optics and Fine Mechanics,  
Chinese Academy of Sciences, Shanghai 201800, China

compiled: October 22, 2018

We investigate the magneto-optical effect of cold atoms in an integrating sphere both experimentally and theoretically. The dependence of magneto-optical rotation angle on the biased magnetic field, the probe light intensity, and the probe light detuning are investigated. The probe light background is blocked and the shot noise is strongly suppressed. This detection scheme may provide a new approach for high contrast cold atom clock and cold atom optical magnetometer.

*OCIS codes:* (020.3320) Laser cooling; (020.1670) Coherent optical effects; (290.2558) Forward scattering.

<http://dx.doi.org/10.1364/XX.99.099999>

## 1. Introduction

Magneto-optics plays an important role in the study of resonant light scattering in the direction of the incident light (forward scattering), whose detection is normally hindered experimentally by the presence of a strong incident-light beam that has identical properties to the forward-scattered light [1]. It also showed the sensitivity higher than could be obtained with absorption measurements [2]. The improved sensitivity of magneto-optical rotation over absorption is due to the almost complete elimination of background light and a corresponding reduction of its influence on the signal noise. Such noise is the main limitation of the absorption techniques. Lin et al. have used faraday rotation to detect the clock signal in a vapor cell to improve its contrast to 90% [3]. We have observed the faraday rotation signal in cold Rubidium atoms in the integrating sphere [4]. Optical Magnetometry techniques with rubidium Bose-Einstein condensates (BEC) for their long-lived, near-stationary collections have recently been demonstrated with high spatial resolution [5, 6]. The Magneto-optical, in particular, the concept of forward scattering signal with cold atoms in an integrating sphere could be used for atomic clock and optical magnetometer.

In this paper, we detect the magneto-optical effects in cold atoms in an integrating sphere for optical magnetometer and atomic clock both experimentally and theoretically. The cold <sup>87</sup>Rb atoms whose temperature is

about 25  $\mu$ K are prepared in an integrating sphere made of glass with a high reflectivity coating of 96% at 780 nm.

## 2. Theory

In this work, the cold <sup>87</sup>Rb atoms are first prepared at the energy level  $5^2S_{1/2}, F = 2$  by the cooling laser and the repumping laser. The FS intensity for weak-intensity probe light can be written as [1]

$$I_{FS} = \frac{1}{4}I_0(e^{-\alpha_+\omega l/c})^2 - e^{-\alpha_-\omega l/c})^2 + I_0e^{(-\alpha_++\alpha_-\omega l/c)^2} \sin^2\left[\frac{(n_+ - n_-)\omega l}{2c}\right], \quad (1)$$

where  $I_0$  is the probe light intensity,  $\omega$  is the angular frequency,  $l$  is the length of the cold atom vapor,  $\alpha_{\pm}$  are the absorption indices and  $n_{\pm}$  are the refractive indices for the  $\sigma^{\pm}$  components of the probe light with detuning, which are given by [7]

$$\alpha_+ = \frac{P^2\Delta N}{\varepsilon_0\hbar} \frac{\gamma}{\gamma^2 + (\Delta + 2\delta)^2}, \quad (2a)$$

$$\alpha_- = \frac{P^2\Delta N}{\varepsilon_0\hbar} \frac{\gamma}{\gamma^2 + \Delta^2}, \quad (2b)$$

$$n_+ = \frac{P^2\Delta N}{\varepsilon_0\hbar} \frac{\Delta + 2\delta}{\gamma^2 + (\Delta + 2\delta)^2}, \quad (2c)$$

$$n_- = \frac{P^2\Delta N}{\varepsilon_0\hbar} \frac{\Delta}{\gamma^2 + \Delta^2}, \quad (2d)$$

where  $P$  is the dipole moment,  $\varepsilon_0$  is the free space permittivity,  $\gamma$  ( $\sim 0.3 \text{ s}^{-1}$ ) is the relaxation rate of the

\* Corresponding author: chenghd@siom.ac.cn

† Corresponding author: liang.liu@siom.ac.cn

ground states,  $\Delta$  is the probe light detuning with resonance,  $\delta$  is the absolute detuning of  $\sigma^\pm$  caused by Zeeman shifts which can be expressed as  $g\mu_B B/\hbar$ , here  $g$  is the Landé g-factor,  $\mu_B$  is the Bohr magneton,  $B$  is the biased magnetic field, and  $\Delta N$  is the population difference between the ground and excited states which approximates to  $N_0\rho(\Omega_l)$  in the weak optical pumping case ( $\Omega_l \ll \Gamma^*$ ,  $\Gamma^*$  is the excited state decay rate), here  $N_0$  is the atomic concentration of the cold atoms, and  $\rho(\Omega_l)$  is the density matrix element representing the population at energy level  $5^2S_{1/2}, F=2$  at dynamic equilibrium which can be obtained by solving the optical Bloch equation [8] and can be given as  $\Omega_l^2/(4\gamma^3\Gamma^*)$ , where  $\Omega_l$  is the probe light's Rabi frequency,  $\Gamma^* = 3.8 \times 10^7 s^{-1}$ , and  $\gamma' = \gamma + (|\Omega_l|^2/2\Gamma^*) \sim \gamma$ . The exponential part in Eq. 1 corresponds to the absorption, and the sine function describes the birefringence. Since the rotation angle is very small, it could be expressed as

$$\theta \approx \frac{I_{FS}}{I_0}. \quad (3)$$

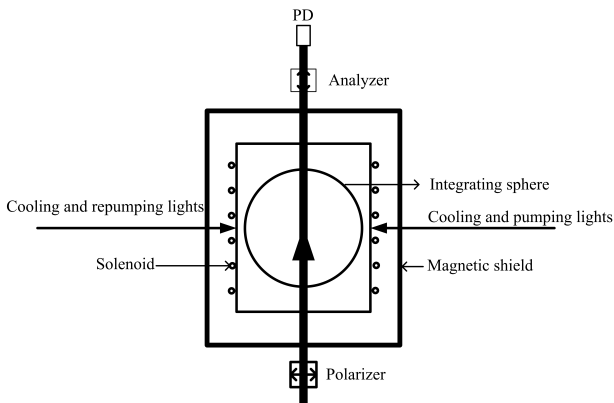


Fig. 1. Experimental setup for the magneto-optical effects detection in cold  $^{87}\text{Rb}$  atoms in an integrating sphere. The integrating sphere and the solenoid are placed inside a cylindrical  $\mu$ -metal magnetic shield to isolate them from external magnetic fields. The solenoid wrapping around the sphere produces the longitudinal magnetic field that provides a quantization axis and lifts the Zeeman sub-level degeneracy. Before and after the integrating sphere and the magnetic shield, a linear polarizer (Glan-Taylor prism) and an analyzer which have orthogonal optical axes, acting as a blocker to the probe light background from the (photo-detector) PD.

Eqs. (1–3) show that the signal detected by the photo-detector (PD) depends on the applied biased magnetic field, the probe light intensity, and the probe light detuning. Therefore the rotation angles' relationships with the above parameters are studied in this work for its applications in atomic clock and optical magnetometer.

The dependence of the rotation angle on the biased magnetic field is linear with  $B$  at small values and then falls off at large fields. Combined with the absorption

and birefringence effects, there will be nonlinear effects in FS at high light intensity and with light detuning. The principal mechanisms are velocity selective modifications of the atomic population distributions by probe light and the light-induced coherences between Zeeman sublevels which operate simultaneously.

### 3. Experimental Details

The experimental setup is shown in Fig. 1. Its inner diameter is 40 mm and the background pressure is maintained at  $10^{-7}$  Pa by a 40 L ion pump (Varian). The Rubidium atomic vapor exists in the sphere between two crossed polarizers in a weak longitudinal magnetic field and the transmitted signal of the forward scattering (FS) depends on the magneto-optical rotation of the polarization plane of the incident linearly polarized probe light without background noise [9, 10], which is a result of the birefringence caused by the opposite displacement of the dispersion curves for the two circular polarizations ( $\sigma^\pm$ ) [1, 11]. The related atomic levels are illustrated in Fig. 2(a). The cold Rubidium atoms are first prepared by the cooling laser (Toptica TA100) locked to the transition of  $5^2S_{1/2}, F=2 \rightarrow 5^2S_{3/2}, F'=3$  and the repumping laser (Toptica DL100) locked to the transition of  $5^2S_{1/2}, F=1 \rightarrow 5^2S_{3/2}, F'=2$ , respectively. Then the probe laser (Toptica DL pro) transition is from  $5^2S_{1/2}, F=2$  to  $5^2S_{3/2}, F'=3$  and passes through a linear polarizer (Glan-Taylor prism) before entering the integrating sphere, which is placed inside a cylindrical  $\mu$ -metal magnetic shield to isolate them from external magnetic fields. The solenoid wrapping around the sphere produces the longitudinal magnetic field that provides a quantization axis and lifts the Zeeman sub-level degeneracy. After the integrating sphere and the magnetic shield, there is another analyzer that is orthogonal to the polarizer, acting as a blocker to the probe light background from the PD. The pumping laser is locked to the transition of  $5^2S_{1/2}, F=2$  to  $5^2S_{3/2}, F'=2$  to keep the atoms in the  $5^2S_{1/2}, F=1$  level. In the experiment, the power of cooling and repumping lights are 130 mW and 5 mW, respectively. The pumping light's power is about 1 mW. The probe light's diameter is 4 mm for detection. The timing sequence of the experiment is shown in Fig. 2(b), both of the cooling time  $t_c$  and the repumping time  $t_r$  are 177.5 ms. The probe light is switched on immediately after the cooling and repumping lights being off and the probe time  $t_{pr}$  is 7.5 ms. Then the pumping light is switched on after the probe laser being on for 4.5 ms for pumping cold atoms to  $5^2S_{1/2}, F=1$  and detecting the leaked background probe light. The pumping time  $t_{pu}$  is 2 ms. In the presence of the weak longitudinal magnetic field, circular polarization light  $\sigma^\pm$  excites the transitions between  $5^2S_{1/2}, F=2, m_F=0, \pm 1, \pm 2$  and  $5^2S_{3/2}, F'=3, m_F=0, \pm 1, \pm 2, \pm 3$ .

### 4. Experimental Results and Discussions

We can calculate the rotation angle versus the applied biased magnetic field, the probe light intensity, and the probe light detuning according to Eqs. (1–3). When the

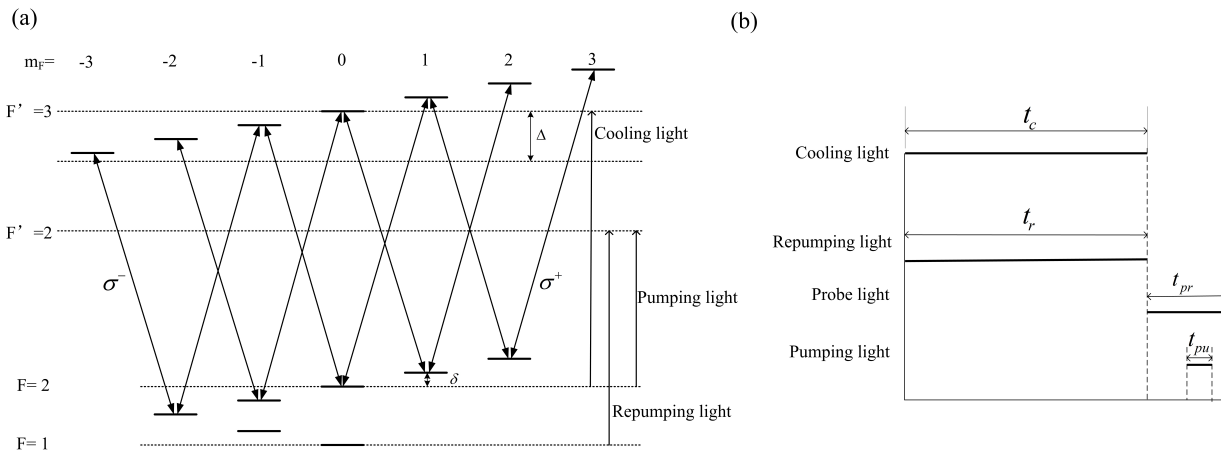


Fig. 2. (a) Energy levels of  $^{87}\text{Rb}$   $D_2$  line interacting with lasers and biased magnetic fields. (b) Timing sequence of the experiment.  $t_c = t_r = 177.5$  ms,  $t_{pr} = 7.5$  ms, and  $t_{pu} = 2$  ms.

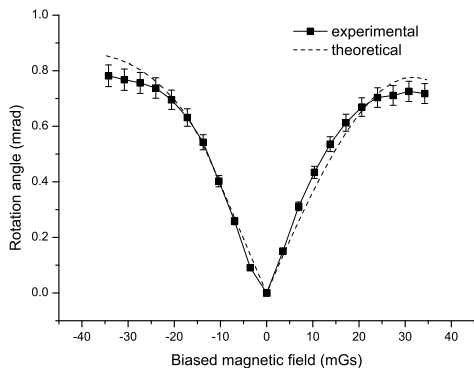


Fig. 3. Experimental (symbol curve) and theoretical (dashed curve) results of the transmitted absolute rotation angle versus the biased magnetic field. The rotation angle  $\theta$  is about symmetrical with opposite magnetic field directions, it is linear with  $B$  at small values of the biased magnetic field, peaks at about 30.8 mGs, and then starts to fall off at larger fields which we didn't measure.

probe light's detuning is -15 MHz and the light's intensity is  $170 \mu\text{W}/\text{cm}^2$ , the transmitted absolute rotation angle versus the biased magnetic field (-34.25 mGs to 34.25 mGs) is shown in Fig. 3. The theoretical results (dashed curve) according to Eq. 3 fit well with the experimental results (symbol curve). Here the calculated curve depends on the energy levels shown in Fig. 2 (a). The rotation angle  $\theta$  is about symmetrical with opposite magnetic field directions. It is linear with  $B$  at small values of the biased magnetic field, peaks at about 30.8 mGs, and then starts to fall off at larger fields which we didn't measure. Then the rotation angle versus the probe light's intensity is shown in Fig. 4 in the case of  $B = 27.4$  mGs, and the probe light detuning is set as 0,  $\pm 15$  MHz, respectively. The dashed line represents the

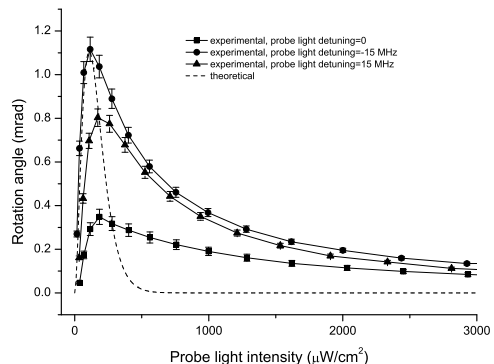


Fig. 4. Experimental (symbol curves) and theoretical (dashed curve) results of the rotation angle versus the probe light's intensity in the case of  $B = 27.4$  mGs, and the probe light detuning is set as 0,  $\pm 15$  MHz, respectively. There are three peaks at around  $114.9 \mu\text{W}/\text{cm}^2$  with different detunings in a descending order at red detuning -15 MHz, blue detuning +15 MHz and 0 detuning (resonance). It then decreases quickly at large intensities.

theoretical result and is consistent with the experiment results (symbol lines). There are three peaks at around  $114.9 \mu\text{W}/\text{cm}^2$  from different probe light detunings in a descending order at red detuning -15 MHz, blue detuning +15 MHz and 0 detuning (resonance). It then decreases quickly at large intensities. There are nonlinear effects appear in FS when the absorption and refractive indices become intensity dependent.

The rotation angle also depends on the probe light detuning (from -45 to 55 MHz), which is shown in Fig. 5 experimentally (symbol lines) and theoretically (dashed line) when the absolute biased magnetic field is fixed at 27.4 mGs and the probe light is  $114.9 \mu\text{W}/\text{cm}^2$  by scanning the light frequency. It is clearly seen that there

are two peaks at detunings of -15 MHz and 10 MHz, respectively, while there is a dip on resonance. The experimental result fits well with the theoretical line, but it is a little different from the theoretical result because the experimental condition is not ideal. In opposite directions of the magnetic fields, the profiles of rotation angles versus the detuning are similar that larger values appear in red detunings. It is consistent with curves of Fig. 4 that the largest rotation angle is at red detuning of -15 MHz while the smallest is on resonance.

Since the Magneto-optical effects (FS signal) are detected in cold  $^{87}\text{Rb}$  atoms, the curve without polarization gradient cooling (stars) is also measured with the same parameters ( $B=27.4$  mGs,  $I_0 = 114.9 \mu\text{W}/\text{cm}^2$ ) at higher temperature than the cooling process with polarization gradient cooling (circles and triangles) [12]. It is clearly seen that the rotation angle is higher at lower temperatures.

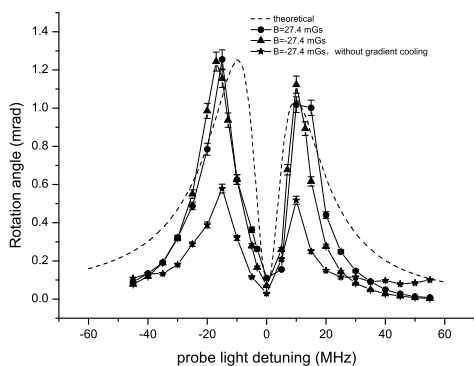


Fig. 5. Theoretical (dashed curve) and experimental (symbol curves) results of the rotation angle versus the probe light’s detuning when the absolute biased magnetic field is fixed at 27.4 mGs and the probe light is  $114.9 \mu\text{W}/\text{cm}^2$ , and the experimental curve without polarization gradient cooling (stars) is detected. There are two peaks at detunings of -15 MHz and 10 MHz, respectively, while there is a dip on resonance.

## 5. Conclusion

We present the magneto-optical effects in cold atoms in an integrating sphere both experimentally and theoretically for high contrast cold atom clock and optical magnetometer. The rotation angles’ (FS signal) relationships with the biased magnetic field, the probe light intensity, and the probe light detuning are investigated. The optimal parameters for the experiment are obtained

at lower cold atom temperature with polarization gradient cooling, the biased magnetic field is 27.4 mGs, the light intensity is  $114.9 \mu\text{W}/\text{cm}^2$ , and the light red detuning is 15 MHz, respectively. This detection scheme may provide a new approach for high contrast cold atom clock and cold atom optical magnetometer.

We thank J. Qian and J. Lin for useful discussions and help in the theory and experiments. This work was supported by the National Natural Science Foundation of China (No. 11034008) and the National High-Tech Research and Development Program (No. 2012AA120702).

## References

- [1] D. Budker, W. Gawlik, D.F. Kimball, S.M. Rochester, V.V. Yashchuk, and A. Weis, “Resonant nonlinear magneto-optical effects in atoms,” *Rev. Mod. Phys.* **74**, 1153–1201 (2002).
- [2] D.A. Church and T. Hadeishi, “Trace-element detection method based on coherent scattering of radiation,” *Appl. Phys. Lett.* **24**, 185–186 (1974).
- [3] J.D. Lin, J.L. Deng, Y.S. Ma, H.J. He, and Y.Z. Wang, “Detection of ultrahigh resonance contrast in vapor-cell atomic clocks,” *Opt. Lett.* **37**, 5036–5038 (2012).
- [4] B.C. Zheng, H.D. Cheng, Y.L. Meng, L. Xiao, J.Y. Wan, and L. Liu, “Observation of faraday rotation in cold atoms in an integrating sphere,” *Chin. Phys. Lett.* **31**, 073701–(1–4) (2014).
- [5] S. Wildermuth, S. Hofferberth, I. Lesanovsky, S. Groth, P. Krüger, J. Schmiedmayer, and I. Bar-Joseph, “Sensing electric and magnetic fields with Bose-Einstein condensates,” *Appl. Phys. Lett.* **88**, 264103–(1–3) (2006).
- [6] M. Vengalattore, J.M. Higbie, S.R. Leslie, J. Guzman, L.E. Sadler, and D.M. Stamper-Kurn, “High-resolution magnetometry with a spinor Bose-Einstein condensate,” *Phys. Rev. Lett.* **98**, 200801–(1–4) 2007.
- [7] M.O. Scully and M.S. Zubairy, *Quantum Optics* (Cambridge University, 1997).
- [8] E. Arimondo, “Coherent population trapping in laser spectroscopy,” *Prog. Opt.* **35**, 257–354 (1996).
- [9] A. Corney, B. P. Kibble, and G. W. Series, “Forward scattering of resonance radiation with special reference to double resonance and level-crossing experiments,” *Proc. R. Soc. Lond. A* **293**, 70–93 (1966).
- [10] W. Gawlik, J. Kowalski, R. Neumann, and F. Träger, “Observation of the electric hexadecapole moment of free Na atoms in a forward scattering experiment,” *Opt. Commun.* **12**, 400–404 (1974).
- [11] C. Wieman and T.W. Hänsch, “Doppler-free laser polarization spectroscopy,” *Phys. Rev. Lett.* **36**, 1170–1173 (1976).
- [12] B.C. Zheng, H.D. Cheng, Y.L. Meng, L. Xiao, J.Y. Wan, and L. Liu, “Development of an Integrating Sphere Cold Atom Clock,” *Chin. Phys. Lett.* **30**, 123701–(1–3) 2013.